Available online at www.sciencedirect.com
ScienceDirect
Ceramics International 37 (2011) 635–639
CERAMICS INTERNATIONAL
www.elsevier.com/locate/ceramint

Porous hydroxyapatite ceramics by ice templating: Freezing characteristics and mechanical properties

Kang Zhao, Yu-Fei Tang *, Ying-Su Qin, Jun-Qi Wei

Department of Materials Science and Engineering, Xi'an University of Technology, Xi'an 710048, PR China

Received 1 July 2010; received in revised form 12 August 2010; accepted 3 October 2010
Available online 28 October 2010

Abstract

Ice templating produces porous hydroxyapatite (HA) scaffolds with a lamellar morphology and aligned channels when using aqueous HA slurries. We investigated the freezing characteristics of HA slurries with regard to the pore structures of the porous HA scaffolds. We found that by increasing the cooling rate, the lamellar spacing decreased. The average lamellar spacing is about 785.7 μm at a cooling rate of 1.3 °C/min. The porous geometry changes from lamella and well aligned channels to a partial dendrite and partially aligned cavities with a decrease in the initial nucleation temperature and an increase in the degree of supercooling. Additionally, we determined the relationship between compressive strength and porosity. The compressive strength of the porous HA scaffolds reach 6.7 MPa at a porosity of 64% and the lamellar spacing is about 124 μm.

Keywords: C. Mechanical properties; Ice templating; Hydroxyapatite; Freezing characteristics

1. Introduction

Hydroxyapatite (HA) is a major inorganic component of hard tissues that are used in the human body, because of its excellent biocompatibility and bone bonding ability [1–3]. Porous HA ceramics have received a great deal of attention in the field of bone regeneration [4–6] since they allow bone cells to penetrate the interconnected pores and to grow on their biocompatible surfaces [7,8]. Controlling the pore structures of the porous scaffold is important for the establishment of channels for histiocytes and nutrients [9,10]. Various manufacturing techniques are available to produce porous HA scaffolds. These methods include the replication of polymer foams [11], the use of pore-forming agents [12] and gel-casting [13]. These methods are suitable for the fabrication of porous scaffolds, but for further investigation, porous ceramics with controllable porosity and open interconnected pores need to be produced.

Recently, ice templating has been used to produce porous HA scaffolds from aqueous HA slurries [14–16]. Among the approaches that use different HA slurry content and a freezing process to control the porosity, the manipulation of interlamellar spacing and compressive strength of the porous HA scaffolds is most promising. Since the pores of the porous HA scaffolds are a replica of the ice structures found after freezing HA slurries [17–19], the freezing characteristics of the HA slurries such as the initial nucleation temperature and supercooling will affect the pore geometry and the interlamellar spacing of the HA scaffolds.

Therefore, in this study we investigated the effects of initial nucleation temperature (T_n) and supercooling (ΔT) to adjust the freezing characteristics of the HA slurries and thus control the pore structures of the porous HA scaffolds. The interlamellar spacing and pore morphologies of the samples were thus investigated. The new results presented here are the temperature curve measurements, clearly showing the supercooling and the nucleation temperature, and the facts that HA samples with very large pores were obtained. We also investigated the quantitative relationship between the porosity and the compressive strength.

2. Experimental procedure

Commercially available hydroxyapatite ($Ca_{10}(PO_4)(OH)_2$, Alfa Aesar Co., Milwaukee, WI) powder and deionized water

* Corresponding author. Postal address: Department of Materials Science and Engineering, Xi'an University of Technology, 5 South Jinhua Road, Xi'an, Shaanxi 710048, PR China. Tel.: +86 29 82312922; fax: +86 29 82312922.
E-mail address: tangyufei1982@gmail.com (Y.-F. Tang).

0272-8842/$36.00
doi:10.1016/j.ceramint.2010.10.003

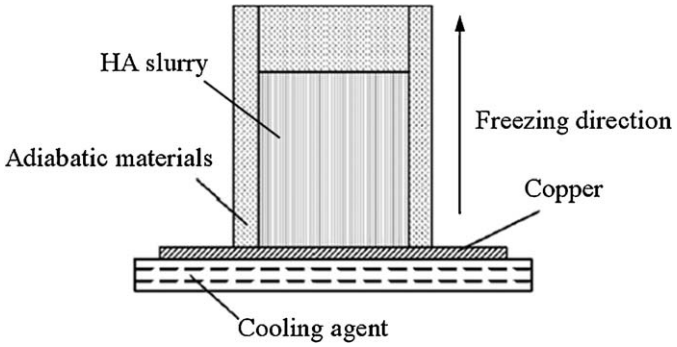

Fig. 1. Brief description of the freezing process.

were used as the ceramic raw material and the freezing vehicle, respectively. In addition, polyvinyl alcohol (PVA, Yakuri Pure Chemicals Co. Ltd., Osaka, Japan) was used as the binder. HA slurries with various initial HA content and 1 wt% PVA were prepared over 4 h by stirring at 60 °C. The slurries were then poured into polyethylene molds with an inner diameter of 15 mm. The molds were placed onto a pre-cooled freeze drier plate (VFD2000G, Boyikang Co. Ltd., Beijing, China) or liquid nitrogen. The samples were frozen by unidirectional freeze casting for 4 h. Since the cooling rate is an important parameter, the temperature of the top and bottom of the samples were determined using an electron thermometric indicator (TH-212, Beijing High-chance High-pech Science Co. Ltd.). The freezing process is shown in Fig. 1. The samples were dried for 48 h to remove the frozen vehicle and then the green bodies were sintered at 1250 °C for 2 h.

The morphology of the porous HA scaffolds was determined by scanning electron microscopy (SEM, 1000B, AMRAY, Cambridge, United States) and binocular stereomicroscopy (SZ61, OLYMPUS, Tokyo, Japan). The lamellar spacing was determined by measuring the cross section of the samples using a digital imaging tool and eight samples were tested to obtain an average value. The porosity of the scaffolds was measured using Archimedes principle. The compressive strength of the scaffolds was measured on cylindrical samples of Φ10 mm × 10 mm using a computer servo to control the material testing machine (HT-2402-100KN, Hungta, Taiwan) with a crosshead speed of 0.5 mm/min. Ten samples were tested to obtain an average value.

3. Results and discussion

Fig. 2(a) shows the morphology of the sintered porous HA scaffold made by a 40 wt% HA content in the initial slurry with the freezing rate of 2.0 °C/min. The HA scaffold with unidirectional aligned channels is lamellar. Macroscopic aligned pores of the HA scaffold are formed almost uniformly over the entire sample. The pore structure of the porous HA scaffold is a replica of the ice structure obtained when freezing HA slurries. These pores were generated during sublimation of the ice and sintering. A dendritic structure is present on the internal walls of the lamellae, as shown in Fig. 2(b). These features reach the adjacent pore walls and, therefore, connecting struts are produced. The aligned channels and the dendritic structure on the internal surface might act as a guiding pattern for cell growth, which will improve the osteoconduction characteristics [20].

The lamellar spacing of the porous HA scaffolds was measured at various freezing rates (1.3, 1.7, 2.0, 2.4, 3.0, 7.0 and 10.0 °C/min), as shown in Table 1. The average lamellar spacing of the porous HA scaffold decreases as the freezing rate increases. The pores are parallel to the direction of heat transfer during solvent crystallization. Aligned channels are produced when the ice crystals are forced to sublimate by adequate drying. At a freeze rate of 10 °C/min, the water in the slurry rapidly reaches a supercooled state and then large quantities of ice crystals are formed. Ice crystal growth is suppressed and they are small in size because of the short freezing time. A porous HA scaffold with a narrow lamellar spacing is thus obtained. At a freeze rate of 1.3 °C/min, a small amount of ice crystals are formed in the HA slurry. Porous HA scaffolds with wide lamellar spacings are obtained since the ice crystals grow over longer freezing times.

Ice crystal growth is dependent on the freezing parameters such as the initial nucleation temperature (T_n) and supercooling (ΔT, the discrepancy between the actual initial nucleation temperature T_n and the equilibrium freezing temperature T_m). The temperature of the slurry was measured periodically when

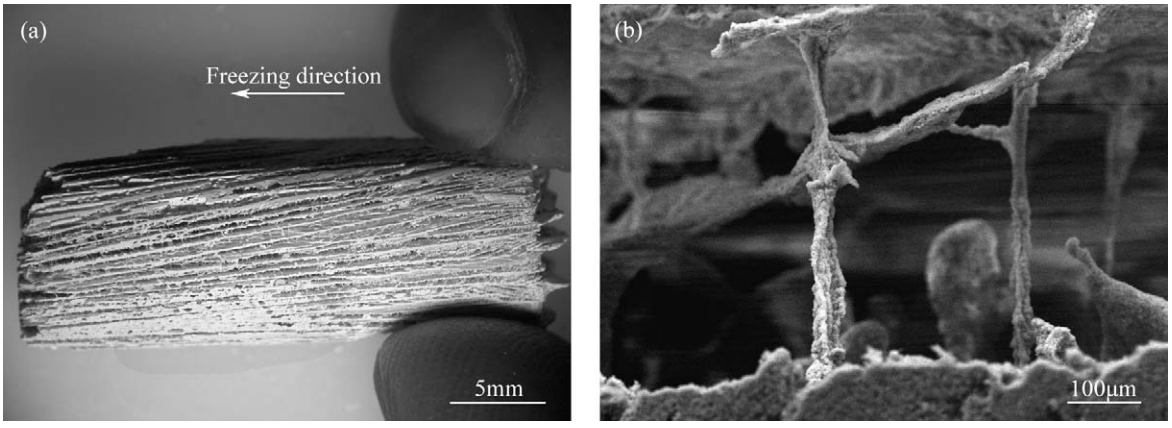

Fig. 2. Morphology of the sintered porous HA scaffolds. (a) Macro morphology and (b) dendritic morphology in the internal walls of the lamellae.

Table 1
Relationship between the average lamellar spacing of the porous HA scaffolds and the freezing rate.

Freeze rate (°C/min)	1.3	1.7	2.0	2.4	3.0	7.0	10.0
Average lamellar spacing (μm)	785 ± 5.7	645 ± 3.9	425 ± 2.7	355 ± 1.6	266 ± 1.8	93 ± 1.6	79 ± 1.3

the temperature of cooling agent is −40 °C and −196 °C respectively, as shown in Fig. 3. Various degrees of supercooling are observed since a temperature difference exists between the slurry and the cooling plate.

The minimum of the curve corresponds to T_n. The temperature (T_m) that corresponds to the flat part of the curve is the freezing point of the slurry. When the temperature of the HA slurry reaches the freezing temperature, no precipitation of ice crystals takes place. A large number of ice crystals are formed while the temperature continues to decrease to a certain freezing temperature. A large amount of latent heat is released during crystallization, which results in an increase in the slurry temperature. With the temperature decreases continually, the temperature of the HA slurry falls again. The degree of supercooling of the HA slurry is 1 °C and 4.5 °C when the temperature of cooling agent is −40 °C and −196 °C, respectively.

Microstructures of porous HA scaffolds at different initial temperatures and degrees of supercooling are shown in Fig. 4.

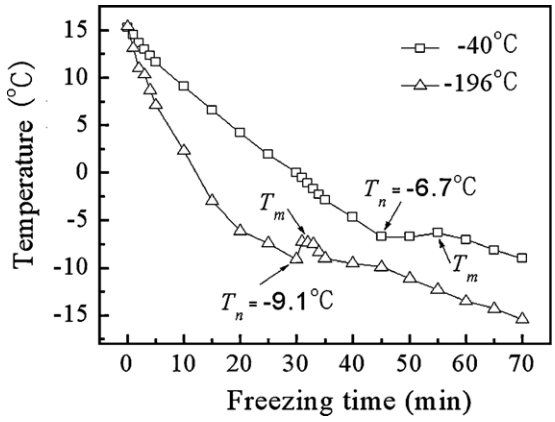

Fig. 3. Freeze curve of the HA slurry at different temperatures.

The porous geometry changes from lamellar at a ΔT of 4.5 °C to a partly aligned cavity at a ΔT of 1 °C. These pores are generated by the sublimation of ice and are aligned along the macroscopic growth direction. When the temperature of the freezing slurry reaches T_n, ice crystals start to nucleate and grow immediately. The ice crystals grow macroscopically in the vertical direction and the HA particles pile up between the ice columns. Additionally, HA powder is expelled by the ice growing between the ice dendrites. The time from the formation of the ice nuclei to the formation of dendritic ice is about 10 s. Dendritic ice grows on the adjacent HA scaffold channel walls at $\Delta T = 4.5$ °C. The freezing behavior of the HA slurry results in the formation of a bicontinuous structure wherein each separate phase (ice crystals and HA powder) are interconnected in an aligned structure of the porous HA scaffold.

The compressive strength of the porous HA scaffolds with different porosity and lamellar spacing was tested and the results are shown in Fig. 5. The compressive strength of the HA scaffold decreased markedly as the porosity increased or the lamellar spacing increased. The compressive strength of the porous HA scaffold reaches 6.7 MPa at a porosity of 64% and the average lamellar spacing is about 124 μm. For porous scaffolds, the compressive strength is directly related to the porosity as shown by the Ryskewith [21] equation:

$$\sigma = \sigma_f e^{-cp} \quad (1)$$

where σ is the strength of the porous ceramic, σ_f is the strength of the dense ceramic, p is the total porosity and $-c$ is a constant.

A logarithmic transformation of Eq. (1) gives:

$$\ln \sigma = \ln \sigma_f - c\,p \quad (2)$$

Therefore, $\ln \sigma$ and p have a linear relationship with $-c$ being the slope of the line. Fig. 5 also shows a linear regression

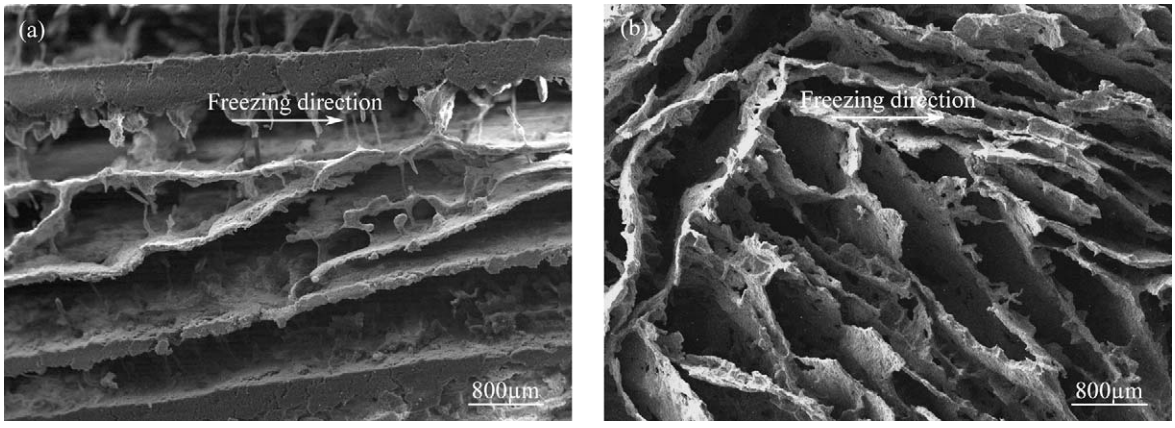

Fig. 4. Misconstruction of the porous HA scaffolds at different ΔT. (a) $\Delta T = 1$ °C and (b) $\Delta T = 4.5$ °C.

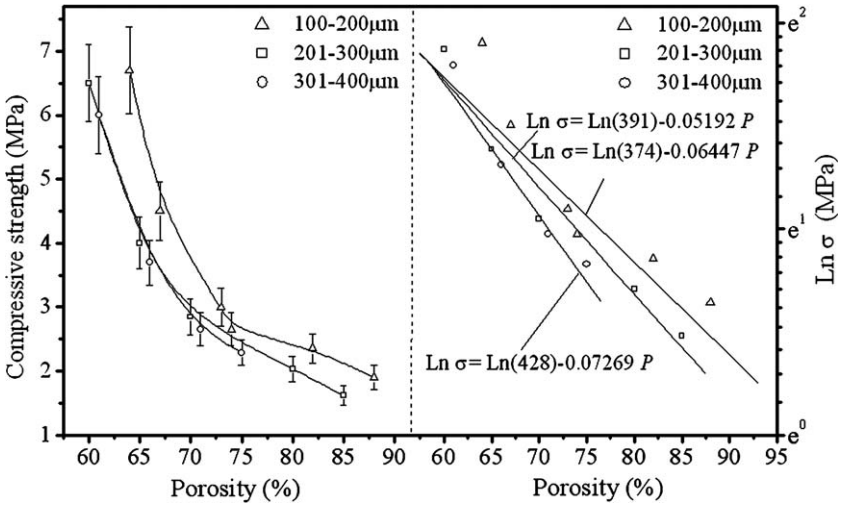

Fig. 5. Compressive strength of the porous HA scaffolds as a function of the porosity. Left: compressive strength vs. porosity. Right: ln σ vs. porosity.

relationship between the porosity and the logarithm of the compressive strength. The fitting equations are as follows:

$$\ln\sigma = \ln(374) - 0.06447\,p \quad 100 - 200\,\textbf{micro;m}\,\mathbf{R^2} = \mathbf{0.957} \tag{3}$$

$$\ln\sigma = \ln(391) - 0.05192\,p \quad 201 - 300\,\textbf{micro;m}\,\mathbf{R^2} = \mathbf{0.954} \tag{4}$$

$$\ln\sigma = \ln(428) - 0.07269\,p \quad 301 - 400\,\textbf{micro;m}\,\mathbf{R^2} = \mathbf{0.968} \tag{5}$$

The obtained σ_f values of 374, 391 and 428 MPa at lamellar spacings of 100–200, 201–300 and 301–400 μm, respectively, are close to the strength of dense HA, as reported in Ref. [22]. The compressive strength of the porous HA scaffold can be predicted by reference to the above equations.

4. Conclusions

In summary, we produced porous HA scaffolds by ice templating using aqueous HA slurries. The freezing characteristics of the HA slurries influence the pore structures of the porous HA scaffolds. The average lamellar spacing of the porous HA scaffolds decrease from 790 to 79 μm with an increase in the freezing rate range from 1.3 to 10 °C/min. As the temperature of cooling agent decreases from −40 °C to −196 °C, the degree of supercooling increases from 1 to 4.5 °C and the initial nucleation temperature decreases from −6.7 °C to −9.1 °C. This results in a change of the porous geometry from an aligned channel to a partial dendrite cavity. The compressive strength of the porous HA scaffold reaches 6.7 MPa for a porosity of 64% and the lamellar spacing is about 124 μm. The relationship between the compressive strength (σ) and the porosity (p) of the porous HA scaffold may be described by the equation $\ln\sigma = \ln\sigma_f - cp$.

Acknowledgments

The authors would like to thank the support from the National Natural Science Foundation of China (No. 50872110) and the Foundation of Excellent Doctoral Dissertation of Xi'an University of Technology (No. 101-211002).

References

[1] Y.P. Lu, M.S. Li, S.T. Li, Z.G. Wang, R.F. Zhu, Plasma-sprayed hydroxyapatite + titania composite bond coat for hydroxyapatite coating on titanium substrate, Biomaterials 25 (2004) 4393–4403.
[2] M. Descamps, J.C. Hornez, A. Leriche, Manufacture of hydroxyapatite beads for medical applications, J. Eur. Ceram. Soc. 29 (2009) 369–375.
[3] M.H. Fathi, A. Hanifi, V. Mortazavi, Preparation and bioactivity evaluation of bone-like hydroxyapatite nanopowder, J. Mater. Process. Technol. 202 (2008) 536–542.
[4] L.H. He, O.C. Standard, T.T.Y. Huang, B.A. Latella, M.V. Swain, Mechanical behaviour of porous hydroxyapatite, Acta Biomater. 4 (2008) 577–586.
[5] S. Iis, K. Jasminder, Preparation and characterization of porous hydroxyapatite through polymeric sponge method, Ceram. Int. 35 (2009) 3161–3168.
[6] S.W. Sofie, Fabrication of functionally graded and aligned porosity in thin ceramic substrates with the novel freeze-tape-casting process, J. Am. Ceram. Soc. 90 (2007) 2024–2031.
[7] J.C. Hornez, F. Chai, F. Monchau, N. Blanchemain, M. Descamps, H.F. Hildebrand, Biological and physico-chemical assessment of hydroxyapatite (HA) with different porosity, Biomol. Eng. 24 (2007) 505–509.
[8] R.R. Hassna, M.Q. Zhang, Preparation of porous hydroxyapatite scaffolds by combination of the gel-casting and polymer sponge methods, Biomaterials 24 (2003) 3293–3302.
[9] H. Wang, Y. Li, Y. Zuo, J. Li, S. Ma, L. Cheng, Biocompatibility and osteogenesis of biomimetic nano-hydroxyapatite/polyamide composite scaffolds for bone tissue engineering, Biomaterials 28 (2007) 3338–3348.
[10] E. Landi, F. Valentini, A. Tampieri, Porous hydroxyapatite/gelatine scaffolds with ice-designed channel-like porosity for biomedical applications, Acta Biomater. 4 (2008) 1620–1626.
[11] I.K. Jun, Y.H. Koh, J.H. Song, S.H. Lee, H.E. Kim, Improved compressive strength of reticulated porous zirconia using carbon coated polymeric sponge as novel template, Mater. Lett. 60 (2006) 2507–2510.
[12] Z. Živcová, E. Gregorová, W. Pabst, D.S. Smith, A. Michot, C. Poulier, Thermal conductivity of porous alumina ceramics prepared using starch as a pore-forming agent, J. Eur. Ceram. Soc. 29 (2009) 347–353.
[13] A.A. Babaluo, M. Kokabi, M. Manteghian, R.S. Mamoory, A modified model for alumina membranes formed by gel-casting followed by dip-coating, J. Eur. Ceram. Soc. 24 (2004) 3779–3787.

[14] S. Deville, E. Saiz, A.P. Tomsia, Freeze casting of hydroxyapatite scaffolds for bone tissue engineering, Biomaterials 27 (2006) 5480–5489.
[15] S. Yunoki, T. Ikoma, A. Monkawa, K. Ohta, M. Kikuchi, S. Sotome, K. Shinomiya, J. Tanaka, Control of pore structure and mechanical property in hydroxyapatite/collagen composite using unidirectional ice growth, Mater. Lett. 60 (2006) 999–1002.
[16] Y. Zhang, K.H. Zuo, Y.P. Zeng, Effects of gelatin addition on the microstructure of freeze-cast porous hydroxyapatite ceramics, Ceram. Int. 35 (2009) 2151–2154.
[17] E. Munch, E. Saiz, A.P. Tomsia, S. Deville, Architectural control of freeze-cast ceramics through additives and templating, J. Am. Ceram. Soc. 92 (2009) 1534–1539.
[18] C. Pekor, B. Groth, I. Nettleship, The effect of polyvinyl alcohol on the microstructure and permeability of freeze-cast alumina, J. Am. Ceram. Soc. 93 (2010) 115–120.
[19] S. Deville, E. Saiz, R.K. Nalla, A.P. Tomsia, Freezing as a path to build complex composites, Science 311 (2006) 515–518.
[20] B.H. Yoon, C.S. Park, H.E. Kim, Y.H. Koh, In situ fabrication of porous hydroxyapatite (HA) scaffolds with dense shells by freezing HA/camphene slurry, Mater. Lett. 62 (2008) 1700–1703.
[21] G. Lu, G.Q.M. Lu, Z.M. Xiao, Mechanical properties of porous materials, J. Porous Mater. 6 (1999) 359–368.
[22] K.J.L. Burg, S. Porter, J.F. Kellam, Biomaterial developments for bone tissue engineering, Biomaterials 21 (2000) 2347–2359.